PTL-2121

Self-Sustained Ultrafast Pulsation in Coupled VCSELs

C.Z. Ning*

Computational Quantum Optoelectronics, NASA Ames Research Center

Mail Stop T27A-1, Moffett Field, CA 94035-1000

Abstract

High frequency, narrow-band self-pulsating operation is demonstrated in two coupled vertical-cavity surface-emitting lasers (VCSELs). The coupled VCSELs provide an ideal source for high-repetition rate (over 40 GHz), sinusoidal-like modulated laser source with Gaussian-like near- and far-field profiles. We also show that the frequency of the modulation can be tuned by the inter-VCSEL separation or by DC-bias level.

Index terms: surface-emitting lasers; optical modulation; millimeter wave modulation; self-pulsing lasers; ultrafast optics.

*email: cning@nas.nasa.gov

High repetition-rate optical signal generation is important for a number of applications [1], including narrow-band data transmissions [2], high bit-rate optical time-devision multiplexing (OTDM) technology for telecommunications [3–5], and millimeter-wave optics [6]. Due to typical long carrier lifetime in a standard diode laser, where direct current modulation is limited to modulation frequency of up to 20 GHz, other means of generation have to be pursued for higher frequency sources. Typically such laser sources are provided by multi-section edge-emitting lasers, such as self-pulsating DFB lasers [7] or other passive and active Q-switching lasers. It is well-known that vertical-cavity surface-emitting lasers (VCSELs) have many advantages over edge-emitting lasers, similar high modulation frequency VCSEL sources should be of great interests for the above mentioned applications.

In a recent paper [8], we showed that, by putting two VCSELs in close proximity, ultrafast directional beam switching can be achieved due to inter-VCSEL coupling. In this paper, we further explore this coupled VCSEL system for the purpose of generating narrow-band high-repetition optical signal. To demonstrate this scheme, we performed a numerical simulation. Our numerical simulation shows that this coupled VCSEL system is ideal for producing Gaussian-like near- and far-field profiles that are modulated in a sinusoidal fashion at a repetition rate over 40 GHz. Furthermore the repetition rate can be tuned by adjusting inter-VCSEL separation or DC-bias level. We believe that such VCSELs sources are potentially useful to replace similar edge-emitting sources in some of the applications mentioned at the beginning.

Our simulation begins with the effective Bloch equations(EBEs) [9], which have been used recently to simulate transverse mode dynamics in VCSELs [10]. The model consists of three coupled equations describing diffraction of laser field, carrier diffusion in the transverse plane, and optical gain and refractive index dynamics represented by an effective polarization P_1:

$$\frac{n_g}{c}\frac{\partial E}{\partial t} = \frac{i}{2K}\nabla_\perp^2 E - \kappa E + \frac{iK\Gamma}{2\epsilon_0\epsilon_b}(P_0 + P_1), \tag{1}$$

$$\frac{\partial P_1}{\partial t} = [-\Gamma_1(N) + i[\delta_0 - \delta_1(N)]]\, P_1 - i\epsilon_0\epsilon_b A_1(N) E \tag{2}$$

$$\frac{\partial N}{\partial t} = \nabla_\perp D_N \nabla_\perp N - \gamma_n N + \frac{\eta J(x,y)}{e} + \\ + i\frac{L\Gamma}{8\hbar}[(P_0 + P_1)^* E - (P_0 + P_1)E^*] \quad (3)$$

where $P_0 = \epsilon_0 \epsilon_b \chi_0(N) E$. The variables and parameters are defined as follows: E is the slowly time-varying complex amplitude of the laser field and N is the 2D carrier density. P_0 and P_1 are complex polarizations of the semiconductor medium induced by the laser field. n_g and n_b are group and phase refractive index of the unexcited semiconductor. c is the speed of light and ϵ_0 is the dielectric constant, all of the vacuum. $K = 2\pi n_b/\lambda$ is the optical wave-vector in the medium, where λ is the wavelength. γ_n is the carrier decay rate. κ is the loss due to cavity transmission and background absorption. It is related to the corresponding decay rate $\tilde{\kappa}$ through $\kappa = \tilde{\kappa} n_g/c$. The value of $\tilde{\kappa}$ is taken as 0.52 per picosecond. The $\nabla_\perp$ represents spatial derivatives with respect to x and y, which are transverse to the propagation direction. δ_0 is the detuning between the reference and bandgap frequencies. The diffusion constant is taken as $D_N = 20cm^2/s$ and the carrier decay constant is assumed a value of one inverse nanosecond. The cavity length L is one half of the wavelength. Gain confinement is represented by the space-dependent current profile $J(x,y)$, which also defines locations of VCSELs. The rest of parameters and the construction of the model equations are given in detail elsewhere [8,9].

The numerical scheme has been described in the past [8,10]. As an example, the simulation is performed for gain-guided VCSELs of 5.6 microns in diameter with edge-to-edge separation of 0.6, 0.8, 0r 1.0 microns. Fig.1 shows snapshots of laser near- (bottom) and far-field (top) intensity profiles for the case of 0.8 micron separation, where a cross-section of the intensity profile along the x-axis (or θ_x-axis) is shown. The two profiles are representative of the coupled VCSEL case considered in this paper. The VCSELs are DC-biased equally and slightly above the threshold of the individual lasers. If the two lasers operate independently without coupling, both are stable at their fundamental mode. However, the mutual proximity gives rise to the oscillatory behavior due to gain coupling, as indicated by the density profile in the bottom part. The two profiles show moments in time when one

of the lobes dominates. In general, the situation is somewhere between the cases shown. Therefore, when either near or far field measurements are made with respect to one of the two lobes, one observes a fundamental-mode-like lobe with its intensity oscillating in time. The frequency of this oscillation is around 42 GHz for this specific case, as we will discuss in more detail in the following. In short, what we have is a Gaussian-like near or far field lobe whose intensity oscillates at over 40 GHz.

To study the effects of inter-VCSEL separation, we considered three values for the edge-to-edge separation. The bottom part of Fig.2 shows power spectra for these cases, where near-field intensity from one of the lasers is taken. As we pointed out [8], the spectral response becomes diminished, if the total output from both lasers are taken due to spatial averaging. As we see in the figure, the peak frequencies decrease from 45, 41.5, to 38 GHz as we increase the separation from 0.6, 0.8 to 1.0 μm. This is easy to understand. As we pointed out, the oscillation is due to inter-VCSEL coupling. As the separation increases, the coupling strength decreases, and thus the oscillation frequency. This property gives us an important design flexibility to tune modulation frequency by adjusting the inter-VCSEL separation. However, it seems unlikely to increase the coupling any further by decreasing the separation much smaller than 0.6. Additional coupling mechanisms, such as antiguiding coupling as demonstrated recently for VCSEL arrays [11,12], are needed to increase the coupling strength further if higher frequency modulation is desired.

Another factor affecting the modulation response is the DC bias level. In the upper part of Fig.2, we compare power spectra at two DC bias levels. The dashed curve corresponds to the near-threshold case as in Fig.1. The solid curve is the power spectrum at bias level 50 percent higher. As a result, the peak frequency shifts by 1 GHz. The reason for this shift is again the increase of coupling between the two lasers due to increased overlap between the two carrier density profiles.

In the cases studied so far, both lasers are DC-biased. The oscillation behavior described above is an example of self-pulsating behavior, seen in lasers with saturable absorber, also known as passive Q-switching. In the following, we consider the effects of current modulation

on the pulsating behavior. As an example, we consider the case in Fig.1., but now with an extra AC bias to one of the lasers. We vary the AC modulation frequency from 1 GHz to 50 GHz as indicated by the square signs in Fig.3, where the response of laser intensity of one of the lasers as a function of modulation frequency is shown. The sinusoidal AC amplitude is 1 percent of the DC level. There are a few features worth mentioning: First, the little peak at 3.5 GHz is the well-known relaxation oscillation (RO) frequency of the individual lasers. The peak around 12 GHz is what we believe to be the RO frequency of the joint system. This needs to be elaborated in some detail: The system we study here is somewhere between a case of two independent lasers and a case of one big laser formed by merging the two. As a result, both the individuality and the collectivity show up in the spectral response. Due to the reduced absorption in the overlap area, the big joint laser is effectively pumped farther away from its threshold and thus has larger relaxation oscillation frequency. A third feature of the response curve is the highest peak around 42GHz, which is more than 15 dB stronger than the response around RO frequency. This peak corresponds to the self-pulsation (SP) frequency. The near and far-field of each individual lasers change at this frequency. The two sidebands around the highest peak correspond to beatings between the SP and RO frequencies.

It is known that frequency locking occurs if a self-pulsating laser is modulated with an AC currents. This is demonstrated in Fig.4, where we plot time series of the integrated intensity over both lasers (upper trace with smaller amplitude) and those of the intensity of one of lasers (lower trace with large amplitude). All the parameters are the same as in Fig.1, except that the DC bias is increased by 50 percent and a AC modulating current is added with an amplitude that is 30 percent of the DC level. In all three cases shown in Fig.4(a), (b), and (c), we choose to start from the same initial conditions, the only difference between them is the modulation frequency. Without modulation (a), we see both traces show strong modulation at the relaxation oscillation frequency around 5 GHz in addition to the SP frequency at 42.5GHz. In Fig.(b) where we modulate at 45GHz, the slow modulation around 5GHz is somewhat diminished, but the small modulation still persists. However,

when we apply a modulation at the SP frequency as in Fig.(c), the slow modulation at RO frequency dies out very quickly within 1 ns. The system is quickly locked to the SP frequency, with a sinusoidal-like temporal waveform.

In summary, we have demonstrated a new approach to generate ultrafast modulation at a rate much higher than the typical RO limited frequency. We investigated the effects of inter-VCSEL separation and the DC bias on the generation of such sources. The study indicates several ways to tune the modulation frequency and to maximize it when necessary. The ultrafast sources we proposed here have a few advantages over existing sources. As VCSELs, such sources have automatically all the advantages of regular VCSELs. In addition, the individual laser intensity shows a Gaussian-like distribution for both the near field and far field. Finally the temporal waveform of modulation pattern is sinusoidal. We believe that such VCSEL sources are important for many of the applications mentioned at the beginning of the paper.

ACKNOWLEDGMENT

The author thanks Peter Goorjian for the computer code that was used for the simulation of this work.

FIGURE CAPTIONS

Fig.1: Snapshots of the near- (bottom) and far- (top) field intensity at two different moments in time showing the Gaussian-like lobes in both near and far fields. Dotted line at the bottom shows an example of the carrier density profile. Both lasers are DC biased slightly above threshold.

Fig.2 Power spectra of one of two lasers under DC bias showing comparison between different DC bias levels (top) and different inter-VCSEL distances (bottom).

Fig.3 Modulation response under sinusoidal modulation with amplitude 1 percent of the DC bias which is slightly above threshold. The inter-VCSEL separation is 0.8 microns. Inset shows an expanded view of the lower frequency range around the relaxation oscillation frequency.

Fig.4 Time traces of the total intensity (upper trace in each figure with small amplitude) and that of the intensity of one of the two lasers (lower trace with large amplitude) for three modulation frequencies 0 GHz (a), 45 GHz (b), and 42.5 GHz (c). Intensity of individual VCSELs shows a sinusoidal-like temporal waveform at the SP frequency.

[1] T. Hoshida, H. Liu, M.Tsuchiya, Y. Ogawa, T. Kamiya, "Subharmonic hybrid mode-locking of a monolithic semiconductor laser", IEEE J. Selected Topics in Quant. Electron., **2**, 514(1996)

[2] R. Nagarajan, S. Levy, A. Mar, and J. Bowers, "Resonantly enhanced semiconductor lasers for efficient transmission of millimeter wave modulated light", IEEE Photon. Tech. Lett., **5**, 4(1993)

[3] R. Barry et al, "All-Optical Network Consortium-Ultrafast TDM Networks", IEEE J. Selected Areas in Communications. **14**, 999(1996)

[4] D.M. Spirit, A Ellis, and P. Barnsley, "Optical Time Devision Multiplexing: Systems and Networks", IEEE Communications Mag., December, 56(1994)

[5] U.Feiste, D. As, and A. Ehrhardt, "18 GHz All-Optical Frequency Locking and Clock Recovery Using a Self-Pulsating Two-Section DFB-Lasers",IEEE Photon. Tech. Lett., **6**, 106(1994)

[6] A. Daryoush, "Optical synchronization of millimeter-wave oscillators for distributed architectures", IEEE Trans. Microwave Tech., **38**, 467(1990)

[7] M. Moehrle, U. Feiste, J. Hoerer, R. Molt, and B. Sartorius, " Gigahertz Self-Pulsations in 1.5 μm Wavelength Multisection DFB Lasers", IEEE Photon. Tech. Lett., **4**, 976(1992)

[8] C.Z. Ning and P. Goorjian, "Ultrafast directional beam switching in coupled VCSELs", (submitted to Applied Physics Letters)

[9] C.Z. Ning, R.A. Indik, J.V. Moloney, "Effective Bloch Equations for Semiconductor Lasers and Amplifiers", IEEE J. Quant. Electr., **33**, pp. 1543-1550, (1997)

[10] C.Z. Ning and P.M. Goorjian, in Feature Issue on "Spatial and Polarization Dynamics of Semiconductor Lasers",eds. G.P.Agrawal, C.Z. Ning, and M. San Miguel, J. Opt. Soc. Am., **B16**, 2072(1999).

[11] D.K. Serkland, K.D. Choquette, G.R. Hadley, K.M. Geib, and A. Allerman, "Two-element phased array of antiguided vertical-cavity lasers", Appl. Phys. Lett., **75**, 3754(1999)

[12] D. Zhou and L.J. Mawst, "Two-dimensional phased-locked antiguided vertical-cavity surface-emitting laser arrays", Appl. Phys. Lett., **77**, 2307(2000)

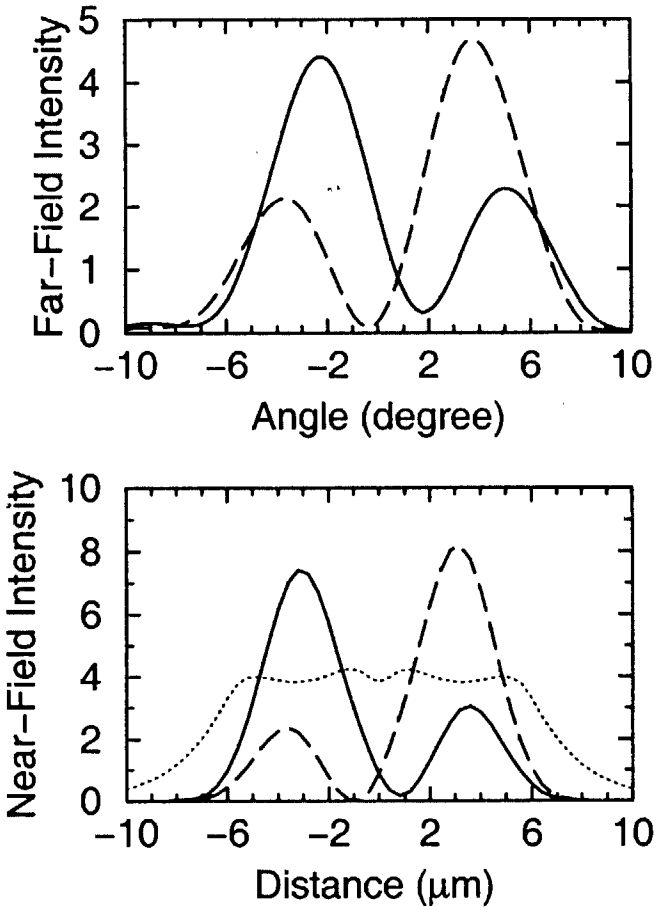
Far-Field Intensity
0
1
2
3
4
5
−10
−6
−2
2
6
10
Angle (degree)
Near-Field Intensity
0
2
4
6
8
10
−10
−6
−2
2
6
10
Distance (μm)

Fig. 1. Ning

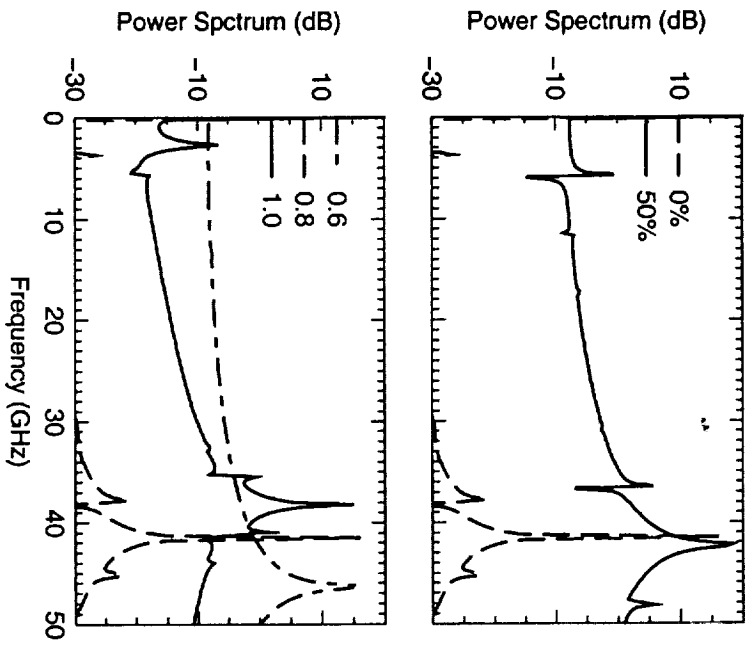
Power Spctrum (dB)
Power Spectrum (dB)
-30
-10
10
0
10
20
30
40
50
Frequency (GHz)
0.6
0.8
1.0
0%
50%

Fig. 2. NMR

Fig. 3. Ning

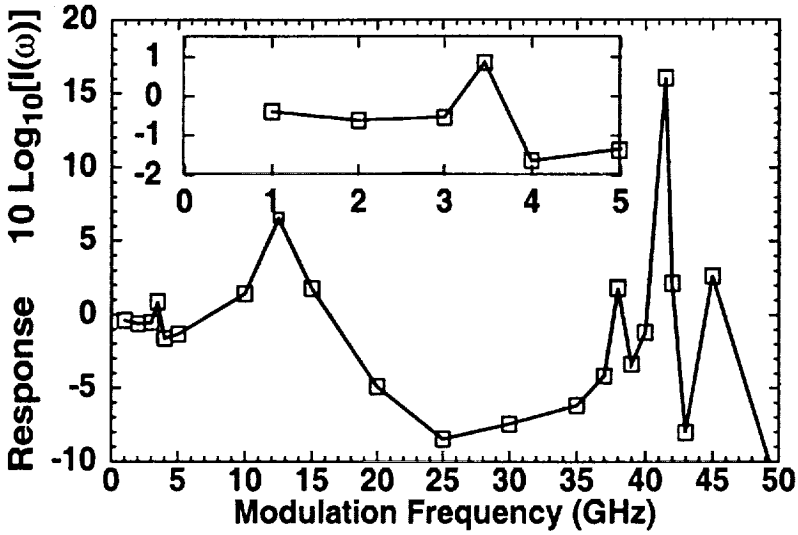
Response 10 Log10[I(ω)]
Modulation Frequency (GHz)
20
15
10
5
0
-5
-10
0
5
10
15
20
25
30
35
40
45
50
1
0
-1
-2
0
1
2
3
4
5

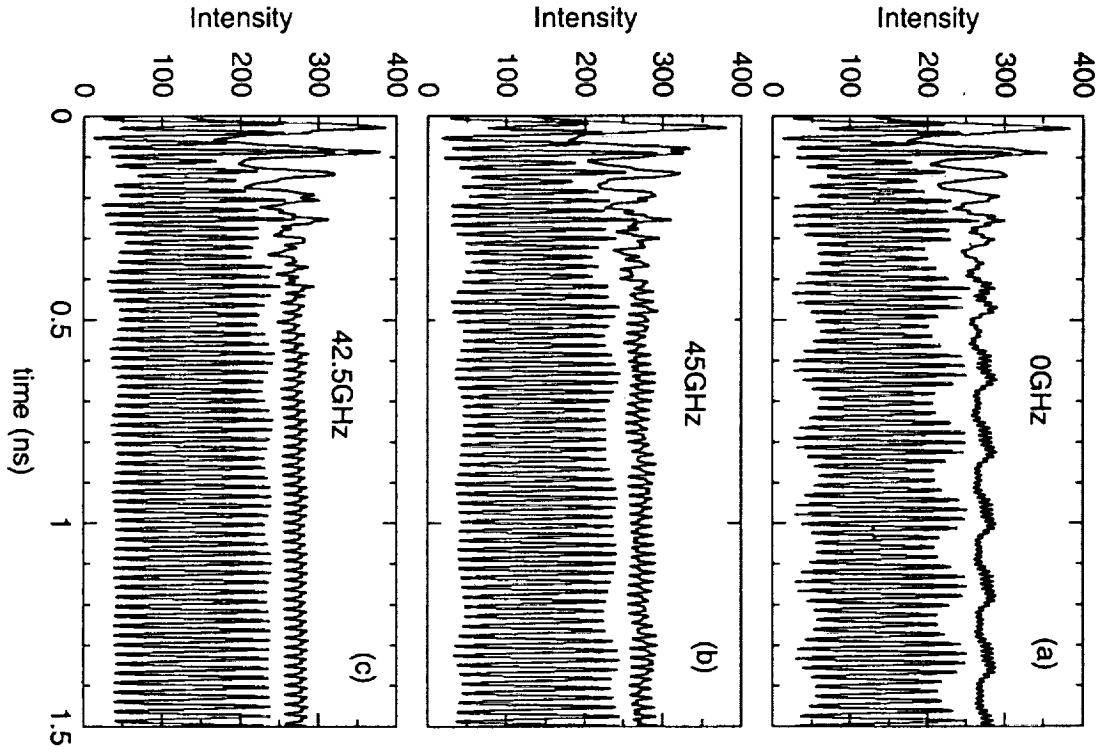
Intensity
0
100
200
300
400
0GHz
(a)
Intensity
45GHz
(b)
Intensity
42.5GHz
(c)
0
0.5
1
1.5
time (ns)

Fig. 4. Ning